Progress In Electromagnetics Research Letters, Vol. 52, 51–56, 2015

High-Selectivity UWB Filters with Adjustable Transmission Zeros

Liang Wang*, Zhao-Jun Zhu, and Shang-Yang Li

Abstract—This letter proposes a novel ultra-wideband (UWB) bandpass filter with compact size and high-selectivity performance. The filter has been studied and implemented through multiple-mode resonator (MMR) using new coupling schemes such as capacitive source-load (S-L) coupling/inductive source-load (S-L) coupling. By properly adjusting the length and width of these stubs, its first four resonant modes can be allocated within the 3.1–10.6 GHz passband, whereas its fifth resonant mode is placed above 16.0 GHz. Two transmission zeros (an inherent transmission zero and an additional transmission zero) can be produced. Moreover, the position of the additional zero can be controlled by adjusting the direct coupling inductance/capacitance. Simulated and measured results are in good agreement indicating that the proposed BPF has a passband (3.0–11.0 GHz)/(2.92–10.6 GHz) and a wide stopband width with 23 dB/25 dB attenuation up to 27.0 GHz. The group delay of the filter is relatively constant and less than 0.65 ns/0.52 ns over the operating pass band.

1. INTRODUCTION

Since the US Federal Communications Commission (FCC) ratified the unlicensed ultra-wideband (UWB) for civil use in 2002 [1], research works on UWB applications have attracted world-wide interest. In the last couple of years, there has been extensive study on UWB RF components especially passive filters, as they play a key role in deciding system response, size and cost effectiveness. UWB filter is required to be developed with compact size, low insertion loss, high out-of-band selectivity, flat group delay, etc. [2–4]. Generally, microstrip filters are realized by implementing discontinuities in design layout such as open-stubs, bends, short-stubs, gaps and resonating structures [5, 6]. In [7], miniature planar UWB filters with circular slots in ground are presented and use a new technique by etching a wideband circular-shape slot resonator in the ground plane of the filters. As reported in [8], multiple mode resonator (MMR) has been used to achieve required UWB bandwidth (2.8 to 11.0 GHz). The MMR is formed by implementing four spur lines and two embedded open-circuited stubs in a tri-section stepped-impedance resonator. In [9] a microstrip UWB BPF with triple-notched bands respectively centered at frequencies of 4.3 GHz, 5.8 GHz, and 8.1 GHz is designed. The triple-notched bands are implemented by coupling a square ring short stub loaded resonator, and any desired frequencies can be generated by varying the designed parameters of square ring resonator. In [10], an advanced UWB filter with wide upper-stopband (the attenuation higher than 20 dB in 11.0–26.0 GHz) is proposed. Then, in [11], triple-notched bands inside the UWB passband are implemented by coupling a square ring short stub loaded resonator to the main transmission line of the initial microstrip UWB BPF.

A new compact UWB BPF with high selectivity filtering characteristics and relatively small size which uses new coupling schemes to suppress the spurious passband and improve the upper stop band is proposed in this letter. We use HFSS 15.0 for simulation, and it is implemented on a substrate with a relative dielectric constant of 10.2 and thickness of 0.635 mm. Remaining part of the paper is divided into three sections. Section 2, describes filters and I/O coupling geometry and analysis. In Section 3,

Received 29 December 2014, Accepted 6 March 2015, Scheduled 16 March 2015
* Corresponding author: Liang Wang (ershao11@126.com).
The authors are with the University of Electronic Science and Technology of China, Chengdu 610054, China.

the measured results of the proposed filter are described and compared with simulated ones. Finally, conclusions are given in Section 4. A good agreement between simulated and measured results ensure the suitability of the proposed BPF for UWB applications.

2. FILTER DESIGN AND I/O COUPLING ANALYSIS

The multiple-mode resonator (MMR) was originally used to design the UWB filter. That UWB filter consisted of stubs-loaded MMR at the center section and two identical coupled-lines located at the left and right sections [4]. Later on, some modified and new kinds of MMR were proposed. In [10], a modified EBG-embedded MMR for UWB BPF with improved upper-stopband performance is explored. In [12], the MMR is formed by attaching three pairs of circular impedance-stepped stubs in shunt to a high impedance microstrip line. However, these MMR-based UWB filters are still limited by the existence of defects, narrow passband in the upper-stopband, and low-selectivity in the passband. To circumvent these problems, a new topology of MMR is utilized to replace the traditional MMR. As depicted in Figure 1, this MMR is formed by attaching three open-circuited stubs alternately with two high-impedance microstrip lines in center. The equal length of these stubs is properly chosen so as to allocate the first four resonant modes of the MMR within the specified passband. When this MMR is driven by weak coupling microstrip lines at two sides, the UWB BPF can be constituted with its equivalent transmission line network in Figure 1. The length and width of the stubs are indicated by H and W, respectively. In this way, the first four resonant modes expect to be relocated within the UWB passband while pushing up the fifth mode to make up a wide upper stopband. Figure 2(a) shows the simulated magnitude of this MMR circuit under weak coupling case. Following the work in [10], it can be understood that the first four resonant frequencies, namely, f_1, f_2, f_3, and f_4 roughly range in the wanted 3.1–10.6 GHz passband, and they can work together to make an ultra-wide passband. In the meantime, the fifth one, i.e., f_5, is located around 16.0 GHz and basically contributes to the first unwanted passband beyond the passband in the initial UWB BPF [10]. In Figure 2(a), S_{21}-magnitude of weak coupled-line is also plotted to show its distributed coupling element. Initially, its first transmission

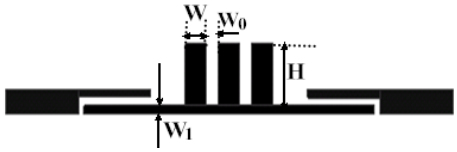

Figure 1. Configuration of the filter with new MMR.

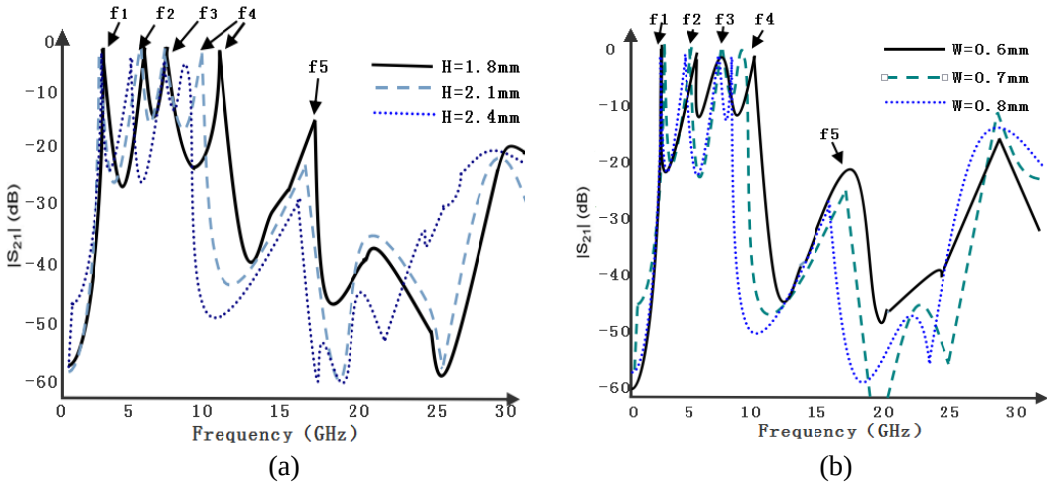

Figure 2. S_{21}-magnitude of the stub-loaded MMR structure in Figure 1 under weak coupling. (a) Versus stub length (H). (b) Versus stub width (W).

zero happens around 13.6 GHz lower than 16.0 GHz. But, this study provides us with a straightforward idea in suppressing this undesired by relocating to this coupling zero. As the stub length is shortened, the first few resonant-mode frequencies are shifted up to different extents as shown. When H decreases, the first four resonant frequencies, i.e., f_1, f_2, f_3, and f_4, increase in an accelerated manner. In particular, the transmission zero appears at 13.6 GHz. Meanwhile, the fifth resonant frequency is almost unchanged at 16.5 GHz. This result ensures us a capability in removing the unwanted passband near the upper cutoff frequency, caused by, in the UWB filter design. Figure 2(b) shows the S_{21}-magnitude frequency response of UWB BPF with the change W, 0.6, 0.7, and 0.8 mm, respectively, as indicated in Figure 1. f_1, f_3 are almost unchanged, and f_2, f_4 have little deviation. We can find that the length of the stubs affects the resonance frequency largely, and the width of the stubs has little impact on it. Then we can adjust the frequency by changing the length and width.

2.1. Filter with Capacitive S-L Coupling

The first microstrip filter example to be described exhibits both an inherent transmission zero T_1 and an additional zero T_2 of the multiple-mode resonator at the upper stopband. Here, the additional zero is generated by capacitive S-L coupling. The locations of the additional zero T_2 may be controlled by adjusting the values of S and L_p. As shown in Figure 3(b), when S decreases from 0.14 to 0.12 and 0.10 mm, the inner transmission zero T_1 almost does not change at 12.5 GHz, but the transmission zero T_2 moves toward the passband edge (15.5 to 13.8 GHz). As well in Figure 3(c), when L_p increases from 2.0 to 2.5 and 3.0 mm, the location of T_1 also changes little around 12.3 GHz, while T_2 moves from 15.8 to 14 GHz. Therefore, the capacitance can be selected to meet the required filter selectivity.

The dimensions are optimized by a full-wave simulator to take all the discontinuities into consideration. The main dimensions are: $W_0 = 0.41$ mm, $W = 0.73$ mm, $S = 0.11$ mm, $H = 1.54$ mm, $L_1 = 3.01$ mm, $L_2 = 6.62$ mm, $L_p = 2.70$ mm.

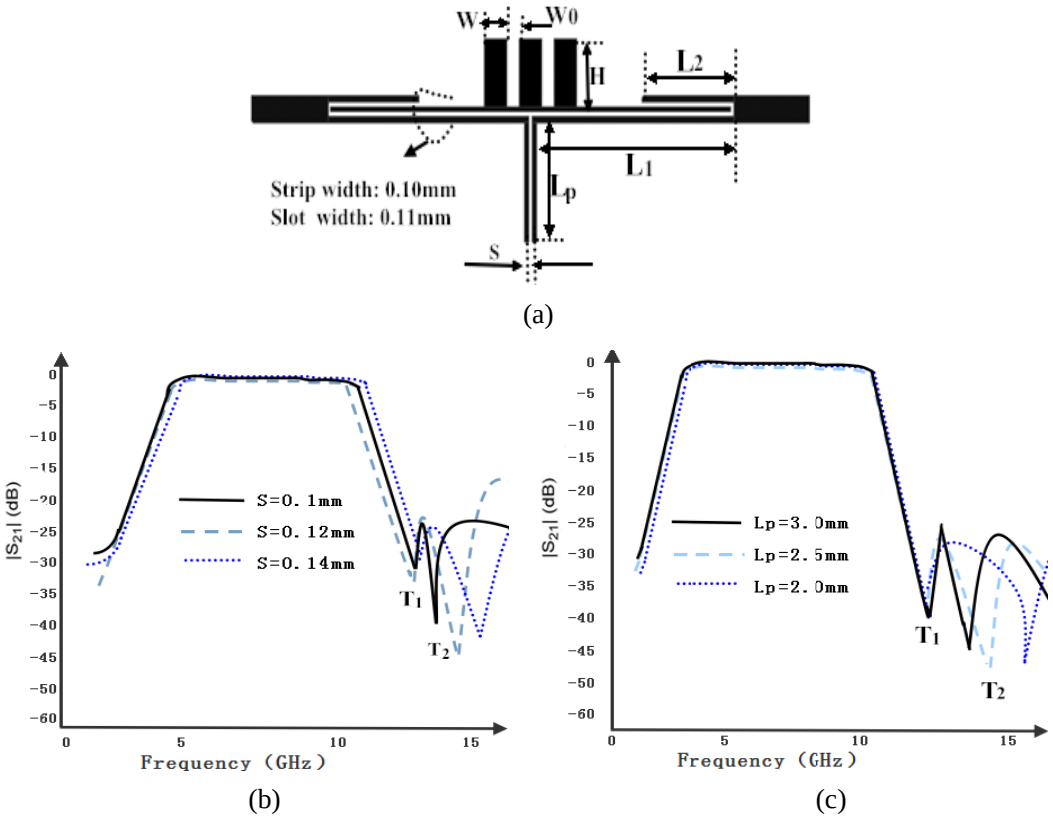

Figure 3. UWB bandpass filter A. (a) Schematic. (b) Simulated scattering parameters versus three S. (c) Simulated scattering parameters versus three L_p.

2.2. Filter with Inductive S-L Coupling

Filter B demonstrates a filtering characteristic with inherent finite frequency zero T_1 at the upper side of the passband while the additional zero T_2 is located at the lower stopband. The inductive S-L coupling is introduced to generate an additional zero at the lower stopband. As shown in Figures 4(b) and (c), when S decreases from 0.2 to 0.1 mm, the transmission zero T_1 of filter B is almost unchanged at 12.2 GHz while the additional transmission zero T_2 increases from 2.5 to 3.0 GHz. When L_p increases from 3.0 to 3.8 mm, the transmission zero T_1 also changes little around 12 GHz; however, T_2 increases from 2.4 to 3.12 GHz. Thus, a sharper fall-off at both low and upper passband edges may be achieved by adjusting S and L_p. The main dimensions are: $W_0 = 0.31$ mm, $W = 0.97$ mm, $S = 0.16$ mm, $H = 1.25$ mm, $L_1 = 4.45$ mm, $L_2 = 7.60$ mm, $L_p = 2.93$ mm, $D = 0.30$ mm.

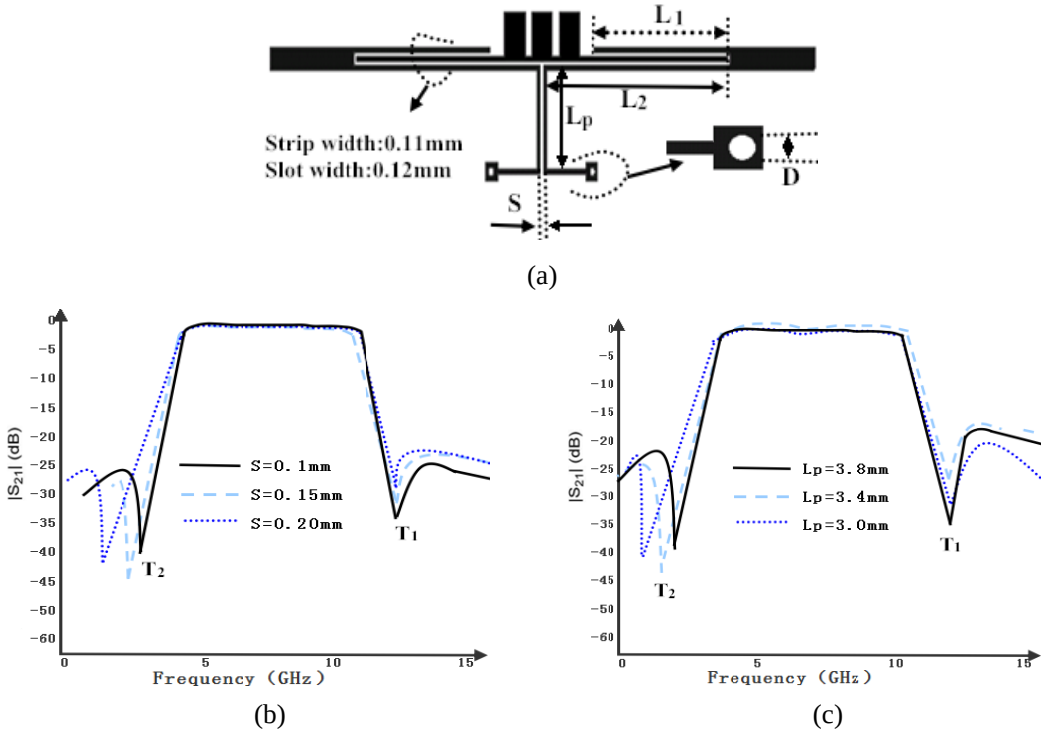

Figure 4. UWB bandpass filter B. (a) Schematic. (b) Simulated scattering parameters versus S. (c) Simulated scattering parameters versus three L_p.

Figure 5. Photographs of the fabricated filters. (a) Filter A. (b) Filter B.

3. MEASUREMENT AND VALIDATION

Two proposed UWB bandpass filters are simulated and fabricated on a substrate Rogers RT6010 with relative permittivity $\varepsilon_r = 10.2$, 0.635 mm of substrate thickness 17 µm of copper thickness and substrate loss of $\tan\delta = 0.002$. The simulation has been carried out by HFSS 15.0 simulator. Figures 5(a) and (b) show photographs of the fabricated filters A and B respectively. The filter size has a total dimension of 19.3 mm × 6.2 mm/24.7 mm × 6.5 mm without connectors.

Figure 6 provides a comparison of the simulated and measured characteristics of the filters. Over the wide frequency range of 1.0 to 28.0 GHz, the predicted and measured results are found to be in good agreement with each other. In the measurement, the lower and higher cutoff frequencies of the UWB passband are equal to 3.011 GHz/2.92–10.6 GHz, respectively. As can be observed in Figures 6(a), (b), the relevant fractional bandwidth achieves about 97.9%/87.9% at the central frequency of 6.85 GHz/6.75 GHz, and the measured insertion loss is found as 0.85 dB/1.6 dB over the UWB passband. We can see that the insertion loss of filter B is about twice as much as filter A, perhaps because filter B is based on inductive S-L coupling, which can be understood as two short stubs. When the short stub is processed, the substrate needs hole metallization which will lead to conductor losses, dielectric losses and etching tolerance, so the insertion loss is greater for filter B. In the passband there are some fluctuations. The measured result presents bad insertion loss in contrast to the simulated ones. The return losses in simulation and measurement are both higher than 20 dB with three transmission poles. Moreover, both insertion loss of filters A and B have small dip in the center of the passband, which may be caused by unwanted harmonic frequency of the resonator, and this phenomenon is more obvious under measurement, which may be caused by unexpected tolerances in fabrication and material

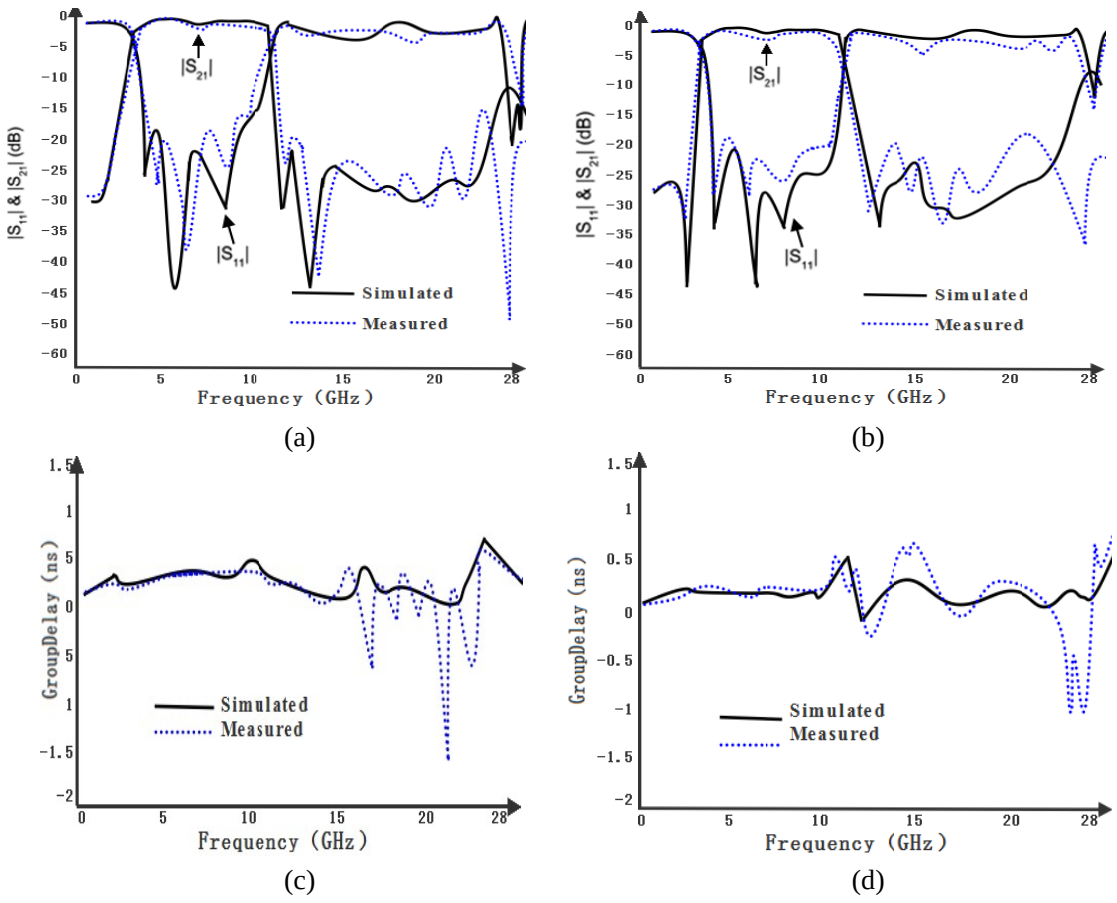

Figure 6. Predicted and measured results of designed filters. (a) Insertion and return losses of filter A. (b) Insertion and return losses of filter B. (c) Group delay of filter A. (d) Group delay of filter B.

parameters.

On the other hand, within the UWB passband, the predicted and measured group delays are both less than 0.65 ns/0.52 ns, varying between 0.20.45 ns /0.2–0.35 ns within the passband, implying good linearity of this proposed UWB bandpass filter. While in stopband, a slight difference is mainly due to the conductor losses, dielectric losses and etching tolerance.

4. CONCLUSION

In this work, two compact UWB bandpass filters have been designed and realized. Two filter prototypes are based on capacitive and inductive S-L coupling. By introducing S-L coupling, the proposed filters exhibit two transmission zeros. It is revealed that a elliptic quasi-response with two adjustable transmission zeros at both skirts can be obtained easily for MMR filter. The proposed structure and design method is verified by the design, fabrication and measurement of two exemplary filters.

REFERENCES

1. FCC, "Revision of Part 15 of the Commission's rules regarding ultra-wideband transmission systems," Federal Communications Commission, Tech. Rep. ET-Docket 98-153, FCC02-48, Apr. 2002.
2. Saito, A., H. Harada, and A. Nishikata, "Development of band pass filter for ultra wideband (UWB) communication," *Proc. IEEE Conf. Ultra Wideband Systems Technology*, 76–80, 2003.
3. Ishida, H. and K. Araki, "Design and analysis of UWB bandpass filter with ring filter," *IEEE MTT-S Int. Dig.*, 1307–1310, Jun. 2004.
4. Zhu, L., S. Sun, and W. Menzel, "Ultra-wideband (UWB) bandpass filters using multiple-mode resonator," *IEEE Microw. Wireless Compon. Lett.*, Vol. 15, No. 11, 796–798, Nov. 2005.
5. Wei, F., P. Chen, L. Chen, and X. W. Shi, "Design of a compact UWB bandpass filter with wide defected ground structure," *Journal of Electromagnetic Waves and Applications*, Vol. 22, No. 13, 1783–1790, 2008.
6. Fallahzadeh, S. and M. Tayarani, "A new microstrip UWB bandpass filter using defected microstrip structure," *Journal of Electromagnetic Waves and Applications*, Vol. 24, No. 7, 893–902, 2010.
7. Naghshvarian-Jahromi, M. and M. Tayarani, "Miniature planar UWB bandpass filters with circular slots in ground," *Progress In Electromagnetics Research Letters*, Vol. 3, 87–93, 2008.
8. Lee, C.-H., I-C. Wang, and L.-Y. Chen, "MMR-based band-notched UWB bandpass filter design," *Journal of Electromagnetic Waves and Applications*, Vol. 22, Nos. 17–18, 2407–2415, 2008.
9. Zhao, J., J. Wang, and J.-L. Li, "Compact microstrip UWB bandpass filter with triple-notched band," *Progress In Electromagnetics Research C*, Vol. 44, 13–26, 2013.
10. Wong, S. W. and L. Zhu, "EBG-embedded multiple-mode resonator for UWB bandpass filter with improved upper-stopband performance," *IEEE Microw. Wireless Compon. Lett.*, Vol. 17, No. 6, 421–423, Jun. 2007.
11. Peng, H., J. Zhao, and B. Wang, "Compact microstrip UWB bandpass filter with triple-notched bands and wide upper stopband," *Progress In Electromagnetics Research*, Vol. 144, 185–191, 2014.
12. Yao, B. Y., Y. G. Zhou, and Q. S. Cao, "Compact UWB bandpass filter with improved upper-stopband performance," *IEEE Microw. Wireless Compon. Lett.*, Vol. 19, No. 6, 27–29, Jun. 2009.